Spring 2010

Signal analysis for multiple target materials through wavelet transforms

Rajat Pashine

Department:

SIGNAL ANALYSIS FOR MULTIPLE TARGET MATERIALS THROUGH WAVELET TRANSFORMS

by

RAJAT PASHINE

A THESIS

Presented to the Faculty of the Graduate School of the

MISSOURI UNIVERSITY OF SCIENCE AND TECHNOLOGY

In Partial Fulfillment of the Requirements for the Degree

MASTER OF SCIENCE IN ELECTRICAL ENGINEERING

2010

Approved by

Dr. Levent Acar, Advisor
Dr. Vittal Rao
Dr. Randy H. Moss

ABSTRACT

Signal identification based on different sensing systems like microwaves, infrared, x-rays and terahertz waves is one of the classic problems in signal processing. Earlier methods had relied mainly on the amplitude spectrum obtained by these sensing techniques mainly due to non-availability of the phase information for the signals. Most of them are based on techniques like absorbance spectrum that requires a reference material's signal for the test material's identification. They are also sensitive to noise and highly dependent on the peak detection algorithms.

Modern equipments with both amplitude and phase information provide an opportunity for time-domain signal based methods that had not been used earlier. In this thesis, the information available through time-domain signals is utilized by the use of different wavelet transform based methods. The methods have been tested for data obtained through the terahertz time-domain spectroscopy (THz-TDS), particularly because of their ability to capture the distinguishing features of the material.

The methods presented here are based on the Continuous and the Discrete Wavelet Transforms. The wavelet transforms have been used to calculate time-frequency energy density in the scale-shift domain. These energy densities have then been used to identify the features described as maxima lines and ridges that are used as features for the purpose of material identification. The methods are found to be useful in the presence of noise require no pre-filtering of the signals as required in most conventional material identification techniques. They also provide a scalable method for increasing accuracy based on the computational power available. All the simulations have been done on MATLAB.

ACKNOWLEDGMENTS

I am very grateful to my advisor Dr. Levent Acar for his guidance during my research. He showed me the direction that I was looking for while giving me the independence to think on my own. He had patiently listened to my ideas and guided me to achieve success in research. The Linear Systems concepts taught by him in his course had laid the foundation of my research work which made it easier for me to absorb the Digital Signal Processing concepts.

I am also grateful to Dr. Vittal Rao for providing me the research opportunity under him. Without the financial support provided by him through research grant, it would have been difficult to me to complete my degree without hardship.

I am also thankful to Dr. Randy H. Moss for serving on my advisory committee and being cooperative. The concepts taught by him as a part of his coursework had also been very useful in the research.

The courses taught by Dr. Steven Grant had further helped me get a good grasp on the concepts of Digital Signal Processing which eventually helped me carry out my research work with ease. Special thanks to Dr. Megan R. Leahy-Hoppa from Johns Hopkins University, Baltimore for providing the test data.

I am greatly indebted to my parents who encouraged me from time to time and taught me to believe in myself. Not to forget other family members and friends who did not let my enthusiasm level fall at any time.

I would also like to thank my friends Keshav Chakravarthy, Dheeraj Singiresu, Soumya De and Pratik Shah for useful discussions and suggestions during my Master's degree.

Lastly I would like to thanks my friends Sarthak, Gurpartap and Bhanu who had always kept the atmosphere jovial and provided moral support.

TABLE OF CONTENTS

LIST OF ILLUSTRATIONS

LIST OF TABLES

1 INTRODUCTION

There has been an increasing number of incidents involving the use of Improvised Explosive Devices (IED's) all around the globe in recent years. IED's are difficult to identify using any of the available techniques such as x-rays, infra-red rays, nuclear imaging alone. They are not able to provide an easily identifiable signature for the components. In contrast, terahertz waves, covering the frequency spectrum from 0.1 to 10 terahertz (wavelengths ranging from 30 micrometers to 3 millimeters), are able to provide a unique signature of the material, [1] . This particular property arises as terahertz signal energies lie in the range of molecular energies of the explosive materials, giving rise to phonon resonance. Similar phenomenon has been exhibited by narcotic drugs on exposure to terahertz waves, providing a way to identify their presence even in concealed form. Moreover, there are a number of other advantages offered by terahertz signals.

- Terahertz waves are non-ionizing, unlike x-rays. This poses minimal health risks to both the person being scanned and the operator.
- Terahertz waves are able to provide high contrast in dielectric materials that are transparent to visible light and have low contrast to x-rays.
- Terahertz imaging uses short femto-second pulses which help in 3-D imaging beneath the soil and other covering materials like plastics, clothes, paper, non polar liquids, etc.
- Microwave imaging and thermal radiation do not provide enough spatial resolution (too high or too low). On the other hand, terahertz waves provide sub-millimeter to millimeter spatial resolution.
- Ground penetrating radars, infra-red rays and x-rays do not have stand-off capabilities and require the user to go near the threat. They also have high false positive rates.
- Optical (Raman Spectroscopy) devices are unable to detect threats concealed under covers.

Conventional metal detectors are usually limited in capability to detecting metal targets, such as ordinary handguns and knives, but not explosive materials. Hence, terahertz waves seem to be a good choice for identification of IEDs. In [2] and [3], the results of terahertz TDS have been compared with the already established Fourier transform infra-red (FTIR) spectroscopy for one of the explosive materials (i.e. RDX) and found to be similar. Moreover, Terahertz TDS has been found useful over a wider range of frequencies (upto 6 THz) over FTIR for a number of explosive materials like RDX, TNT, HMX and PETN in [4]. These materials have been discussed in the appendix.

Most of the material identification techniques using terahertz signals are based on frequency domain analysis [5]. In most of these, the approach has been to find out the dominant frequencies with high absorption peaks and use them as classification features, [4]. Other approaches involve the determination of first derivative absorption spectrum, absorption coefficient and refractive index for purpose of classification, [3]. Parameter analogous to absorption coefficient has also been used in [6] to distinguish between materials using terahertz signals.

Methods involving the use of blind source separation techniques such as Independent Component Analysis (ICA) and constrained ICA (cICA) have also been proposed to find out the proportion of the target material present in a mixture, [7]. However, such techniques require a signal for calibration and are very sensitive to noise. The methods presented in this thesis try to overcome those disadvantages by the use of wavelet transforms.

Mittleman et al. in [8] had proposed that terahertz waveforms share similarities like limited bandwidth and localization in time and frequency, that might prove wavelet analysis as an important analysis tool for terahertz waveforms. Their work also suggests that a wavelet multi-resolution analysis may be a fast and efficient technique to distinguish between different materials. In [6], Shopov et al. mentioned that a non-stationary signal like the terahertz signal often has short lived high frequency feature and long lived low frequency features, which requires an analysis tool to resolve high frequency content in time and as well as low frequency content in frequency. A wavelet-based analysis offers exactly the same advantages.

In [9] and [10], a wavelet denoising technique is used for preprocessing the raw data in order to improve the classification accuracy. In [6], a wide band cross ambiguity function similar to wavelet transform is used to distinguish between materials. Continuous Wavelets Transforms (CWT) have also been used in mass spectroscopy for improved peak detection for the purpose of material identification, [11]. In [12], a Discrete Wavelet Transform (DWT) based approach is used to derive attributes (features) for material classification based on ultrasonic echo signals.

Fewer efforts have been put for using the CWT and the DWT for the purpose of material identification even though the DWT has been used in the preprocessing stages. This thesis presents methods to derive features from the CWT and the DWT coefficients that could be used to classify materials from the time domain signals obtained through the terahertz imaging. The CWT is a non-orthogonal and redundant transform that offers additional properties of shift-invariance and provides better performance than the shift-variant DWT. The identification process has been applied to signals obtained from pure target materials.

The merits of the methods suggested in this thesis are (a) applicability to time domain signals obtained from different sensor systems/hardware (b) applicability to narrow-band as well as wide-band signals.

Section 2 comprises of the wavelet transform related concepts, for both continuous and discrete-parameter wavelet transforms as well as the discrete wavelet transform. The advantages of wavelet transforms over the Fourier transforms and the short-time Fourier transforms have been discussed. The section also describes the properties of the wavelets and the wavelet transforms. Different wavelet families available for analysis have also been listed with short descriptions.

Section 3 starts with the problem of material identification and the classic methods that have been used in the past. This section presents the methods using CWTs that have been used to extract features based on the maxima lines and ridges. These features are found out using local maxima points based on time-frequency energy distribution which have not been reported earlier. The classification of the materials using the extracted features has also been discussed.

Section 4 discusses the material identification based on earlier DWT methods as well as the developed methods. The presented method uses all the frequency

sub-bands (group of frequency bands) decomposed at a given level, and derives the features from those signals after rearranging the sub-band data in a operable manner.

Section 5 depicts the results obtained after the application of the developed methods applied to the terahertz signals. Section 5.2 discusses the identification based on features derived using CWTs considering both non-shifted and shifted versions of the time signals. Section 5.3 discusses the identification based on the features derived using DWTs. Shifted versions of DWTs are inapplicable because of the shift variant nature of the DWT transform.

Finally, Section 6 ends with the concluding remarks about the results and the suitability of the developed methods under different conditions.

2 WAVELET TRANSFORM

The advantages offered by wavelet transforms over the Fourier transform (FT) and the short time Fourier transform (STFT) are discussed in this section. The concepts of the STFT are extended to wavelet transform. The continuous wavelet transform, the discrete parameter wavelet transform as well as the discrete wavelet transform are described. Important properties of wavelets as well as wavelet transforms are discussed. Lastly, a brief description of some wavelet families is given.

2.1 BACKGROUND OF WAVELET TRANSFORMS

The conventional methods for material identification have involved the use of Fourier transform for analysis. The Fourier transform helps in the resolution of the signals in the frequency domain. However, the time/shift information is totally lost in such a transform, that otherwise could be useful. An approach to overcome this shortcoming is to use a windowing function on the time signal and then apply the Fourier transform methods. Such a technique is called the short time Fourier transform or windowed Fourier transform (WFT). Since all the time frequency transforms are limited by the Heisenberg's uncertainty principle, this approach may only give a fixed time-frequency resolution.

A wavelet transform gives an advantage over both the FT and the STFT that the resolution window can be changed through the variation of parameters called scaling factor (or scale) and the shift. A scaling factor serves the purpose of compressing/expanding the windowing function. This process allows small scales (corresponding to smaller windows) to capture high frequency components within the window. Larger scales on the other hand extend over a relatively large portion of the signal being analyzed and tend to capture the low frequency characteristics. The windowing function in this case is called a wavelet. Some of the important properties of wavelets are as given below.

1. **Zero average value**: The average value of a wavelet $\psi(t)$ over time is zero.

$$\int_{-\infty}^{\infty} \psi(t)\, \mathrm{d}t = 0. \tag{2.1}$$

2. **Square Integrability**: The wavelet function is square integrable.

$$\int_{-\infty}^{\infty} |\psi(t)|^2 \, \mathrm{d}t < +\infty. \tag{2.2}$$

2.2 CONTINUOUS WAVELET TRANSFORM

The continuous wavelet transform function $\mathcal{W}^{\psi}_{(a,b)}$ for a time signal $x(t)$ using a wavelet function $\psi(t)$ is given by

$$\mathcal{W}^{\psi}_{(a,b)} = \frac{1}{\sqrt{a}} \int_{-\infty}^{\infty} x(t) \psi^* \left(\frac{t-b}{a} \right) \mathrm{d}t \quad \forall a, b \in R, \tag{2.3}$$

where a is the scale variable, b is the shift variable and R is the set of real numbers. Here $\psi^*(t)$ is the conjugate of the wavelet function $\psi(t)$. For real-valued wavelets, $\psi^*(t) = \psi(t)$.

The function $\psi(t)$ in Equation 2.3 is called the mother wavelet and corresponds to an undilated (uncompressed) windowing function. A daughter wavelet can be created by the compression/expansion as well as shifting of the mother wavelet. The mathematical expression for a daughter wavelet $\psi_{(a,b)}(t)$ is described by

$$\psi_{(a,b)}(t) = \frac{1}{\sqrt{a}} \psi \left(\frac{t-b}{a} \right). \tag{2.4}$$

The reconstruction of the time signal back from the wavelet coefficients is subject to the following admissibility condition

$$\mathrm{C}_{\psi} = \int_{0}^{\infty} \frac{\left| \hat{\psi}(\omega) \right|^2}{\omega} \mathrm{d}\omega < +\infty, \tag{2.5}$$

where C_{ψ} is a constant that is fixed for a particular wavelet $\psi(t)$, $\hat{\psi}(\omega)$ is the Fourier transform of the wavelet $\psi(t)$ and ω is the frequency. The existence of admissibility condition allows the reconstruction of the original signal, such that

$$x(t) = \frac{1}{\mathrm{C}_{\psi}} \int_{a=0}^{\infty} \int_{b=-\infty}^{\infty} \left(\frac{1}{|a|^2} \right) \mathcal{W}^{\psi}_{(a,b)} \ \psi_{(a,b)}(t) \, \mathrm{d}b \, \mathrm{d}a. \tag{2.6}$$

Some important properties of the continuous wavelet transform are given [13] in the next section.

2.3 CONTINUOUS WAVELET TRANSFORM PROPERTIES

1. **Linearity**: The continuous wavelet transform follows the property of linearity, i.e.

$$\mathcal{W}^{\psi}_{(a,b)}\Big(\alpha x_1(t) + \beta x_2(t)\Big) = \alpha\left(\mathcal{W}^{\psi}_{(a,b)} x_1(t)\right) + \beta\left(\mathcal{W}^{\psi}_{(a,b)} x_2(t)\right) \tag{2.7}$$

   where $\mathcal{W}^{\psi}_{(a,b)}$ is the CWT function calculated for the parameters a and b with the wavelet $\psi(t)$, and α and β are scalars.

2. **Translation**: The CWT operator is translation (shift) invariant. This property implies that the CWT of a time-shifted signal is the same as that of the original signal, but shifted along the shift (b) axis. This property has been utilized in Section 3 where both the shifted and non-shifted versions of the signals have been used.

$$\mathcal{W}^{\psi}_{(a,b)}\Big(x(t-\tau)\Big) = \mathcal{W}^{\psi}_{(a,b-\tau)}\Big(x(t)\Big). \tag{2.8}$$

3. **Energy density in time-scale domain**: The energy density in time -scale domain of a time domain signal obtained though the CWT is a three dimensional surface that varies as a function of the shift and the scale parameters. These surfaces are a measure of the distribution of energy present in the signal as time and frequency vary. The energy density in time-scale domain using a wavelet $\psi(t)$ is given by

$$\xi^{\psi}_{(a,b)} = \frac{\left|\mathcal{W}^{\psi}_{(a,b)}\right|^2}{\mathrm{C}_{\psi}\,|a|^2}. \tag{2.9}$$

   where C_{ψ} is defined in Equation 2.5.

4. **Maxima lines**: The CWTs have the advantage that they can be used to find out the regions in a signal where the signal or its derivatives display abrupt

changes. This can be done by analyzing some special lines where the modulus of the CWT is concentrated as pointed by Haase et al. in [14]. Such lines are referred as the maxima lines. Maxima lines are obtained from the partial derivative of the CWT function along the direction of the shift parameter.

5. **Ridges**: Another feature of the CWT is its ability to decompose vibrations into their natural frequency components. If the FT of the analyzing signal concentrates near a fixed frequency, the modulus of the CWT tends to concentrate near a series of curves called ridges. Ridges are obtained by partial differentiation of the CWT function along the direction of the scale parameter.

Determination of Maxima lines and Ridges: The calculation of the maxima lines and ridges is performed by first evaluating the CWT for a discrete set of mesh points (a_i, b_j) where i, j are integers. Local maxima are next determined either for a constant scale a_i or a constant time b_j. An additional chaining algorithm is then used to connect the points of interest.

2.4 DISCRETE PARAMETER WAVELET TRANSFORM (DPWT)

In Equation 2.3, both the shift and the scale are continuous variables. This process clearly results in a redundancy in the CWT representation. It is possible to completely reconstruct the signal $x(t)$ if the wavelet transform coefficients have been sampled densely enough, [15] . The sampling is done through a discretization process, such that the signals are still continuous in time, but the scale and the shift variables are discretized.

For $a = a_0^m$ and $b = nb_0a_0^m$, where m and n are integers, the DPWT coefficients are given by [16]

$$\mathcal{P}^{\psi}_{(m,n)} = \int_{-\infty}^{\infty} x(t)\psi_{m,n}(t)\,\mathrm{d}t \tag{2.10}$$

where $\psi_{m,n}(t) = a_0^{-m/2}\psi(a_0^{-m}t - nb_0)$ and a_0, b_0 are the constants that determine the sampling intervals.

The signal $x(t)$ can now be reconstructed from the basis functions $\psi_{m,n}(t)$ through the reconstruction formula

$$x(t) = c_\psi \sum_m \sum_n \mathcal{P}^{\psi}_{(m,n)} \psi_{m,n}(t) \tag{2.11}$$

where c_ψ is some constant dependent only on $\psi(t)$. The perfect reconstruction and orthogonality of the DPWT is subject to proper choices of a_0 and b_0.

2.5 DISCRETE WAVELET TRANSFORM (DWT)

The discrete wavelet transform is orthogonal unlike the continuous wavelet transform. The CWT serves as an analysis tool and can be seen as a redundant transform in continuous time with continuous scale and shift parameters with dilated and shifted wavelets as the basis functions. The DWT on the other hand is an orthogonal transform with discrete (dyadic) scales and shifts. The basis functions for this transform are the scaled and dilated versions of the wavelet functions ($\psi(t)$) and scaling function ($\phi(t)$). The scaling function helps determine the signal approximation coefficients. These functions are characteristics only to the orthogonal wavelets, [12].

From a frequency domain perspective, wavelets tend to serve as high pass filters and the scaling function tends to act as a low pass filter. The net effect of these properties is that the scaling function and the wavelet function end up spanning the complete spectrum of frequencies.

The DWT serves to decompose the signals into sub-bands. An important feature of the DWT is that it can be implemented using digital filter banks rather than using the basic definition of the wavelet transform. Digital filter banks for wavelets are a set of four filters that can be used to analyze and reconstruct the signals. Two of these filters are used for analysis and consist of a pair of low-pass and high pass filters. Correspondingly, there is a pair of low-pass and high -pass filters for the reconstruction of the signals. These filters are called quadrature-mirror filters (QMFs). An important property of these filters is that they satisfy the perfect reconstruction condition. In other words, when a signal is passed through a set of QMFs, it can be reconstructed without any loss of information.

The equivalence of the implementation of the discrete wavelet transform and use of quadrature-mirror filters for signal analysis is derived through the concepts of Frames and Multi-Resolution Analysis (MRA). The theory of frames is a generalization of the orthonormal decomposition principle and plays an important role in determining the orthogonal nature of the wavelet transform.

The idea of multi-resolution analysis is similar to sub-band decomposition where a signal is divided into a set of frequency bands. The low-pass and high-pass filters along with decimation decompose the signal into its sub-band components. There can be multiple topologies for the sub-band decomposition. Some of the most common are the binary tree and the logarithmic tree decomposition. Figure 2.1 illustrates the use of filter banks for the decomposition of a band limited signal.

Another concept connecting the wavelets and filter banks is that multiple iterations of the low-pass filter leads to the scaling function. Similarly, the multiple iterations of the high-pass filter leads to the wavelet function, [17]. As a result, the discrete wavelet transform can be implemented efficiently through the use of filter banks.

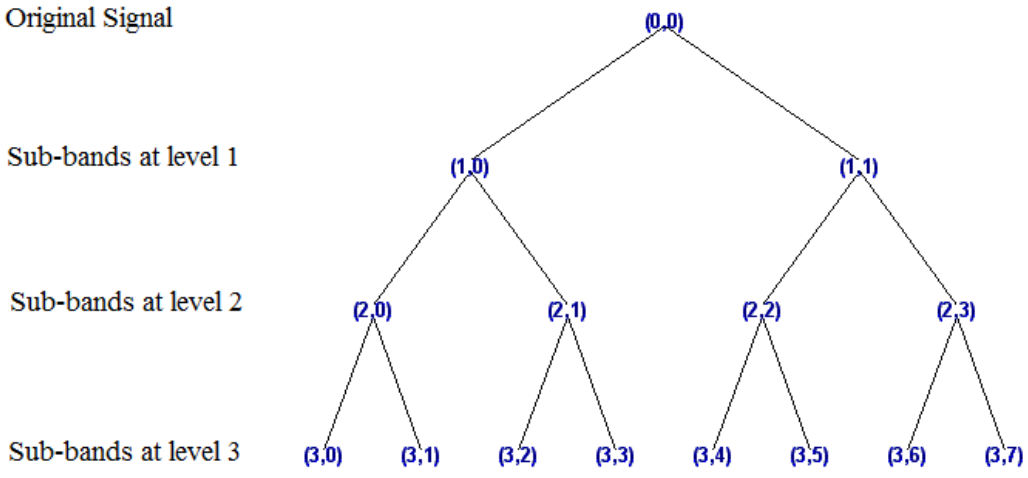

Figure 2.1. Sub-band decomposition view of discrete wavelet transform using filter banks.

2.6 ADDITIONAL PROPERTIES OF WAVELETS

The choice of a particular wavelet for an application depends on the following properties of the wavelets, [5].

1. **Support width**: The support of a wavelet is the range of values for which the wavelet function is non zero. Compact support (finite support width) for a wavelet means that whenever the function is not defined, it will have a value of zero. Compact support is a measure of the temporal localization of the wavelet.

2. **Number of vanishing moments**: A wavelet $\psi(t)$ has p vanishing moments if

$$\int_{-\infty}^{\infty} t^k \psi(t)\, \mathrm{d}t = 0 \text{ for } 0 \leq k < p. \tag{2.12}$$

   This property implies that the wavelet is orthogonal to any polynomial of degree $p-1$. A wavelet with many vanishing moments gives small coefficients when it is used to analyze low frequencies. The number of vanishing moments is related to the number of oscillations of the wavelet; the more the number of vanishing moments, the more the wave oscillates. If a wavelet has p vanishing moments, then its support must be at least $2p-1$, and increasing the size of the wavelet increases the number of computations.

3. **Regularity**: The order of regularity of a wavelet is the number of its continuous derivatives. To have a regularity greater than k, a wavelet must have at least $(k+1)$ vanishing moments. A high order of regularity is required to encode smooth signals. The regularity condition requires the mother wavelet to be locally smooth and concentrated in both time and frequency.

4. **Orthogonality**: Orthogonality of the wavelet functions brings conciseness and speed to the analysis at the cost of shift invariance. In the context of the discrete wavelet transforms, this implies orthogonality of the analysis and synthesis filter banks. Orthogonality is particularly important for signal compression. Orthogonality in the wavelet transform is similar to the sampling theorem. With orthogonal wavelets, it is possible to critically decompose the signals and still be able to reconstruct the signal perfectly. Orthogonal wavelets give the most

compact representation of the signal and provide a way to implement wavelet transforms using filter banks. Orthogonal wavelets give orthogonal matrices and perfect reconstruction, [17].

5. **Bi-orthogonality**: Biorthogonality of wavelets provides both symmetry and compact support though two sets of wavelets, one for analysis and another for synthesis. Symmetry is incompatible with orthogonality which might be required for linear phase. Symmetry is useful in avoiding dephasing, especially in image processing. In terms of digital filter banks, this means that the analysis and synthesis filter-banks are not the transposes of each other. Biorthogonal wavelets give invertible matrices and perfect reconstruction, [17].

6. **Complex or Real**: Complex wavelets are useful when analysis of the phase of time signals is important. For most applications, real wavelets are sufficient for analysis.

2.7 FAMILIES OF WAVELETS

Based on the above listed properties, different families of wavelets have been described. A brief description about these is given below:

1. **Haar wavelets**: The Haar family of wavelets is the simplest of all wavelets. The Haar wavelet function is the only wavelet function which is both linear phase characteristics and orthogonality.

2. **Daubechies wavelets**: These are compactly supported wavelets with extremal phase and the highest number of vanishing moments for a given support width. Associated scaling filters are minimum-phase filters. They do not have any analytic form.

3. **Coiflets**: These are compactly supported wavelets with the highest number of vanishing moments for both the wavelet and the scaling functions for a given support width. They do not have any analytic form.

4. **Bi-orthogonal wavelet**: Bi-orthogonal wavelets have two sets of wavelets; one for analysis and another for reconstruction. These wavelets provide both symmetry and orthogonality.

5. **Symlets**: These are compactly supported wavelets with the least asymmetry and the highest number of vanishing moments for a given support width. The associated scaling filters are near linear-phase filters. These wavelets are obtained by modifying the Daubechies wavelets. They do not have any analytic form.

6. **Meyer wavelet**: Meyer wavelet is defined in the frequency domain. This wavelet does not have finite support but approaches to zero as time approaches to infinity and decays faster than any inverse polynomial. Meyer wavelet is infinitely differentiable. This wavelet ensures orthogonal analysis.

7. **Morlet**: The mother wavelet function is given by
$$\psi(t) = Ce^{-t^2/2}\cos(5t)$$
for some constant C. This wavelet has infinite support, but its effective region is the closed interval [-4,4]. It is usually implemented using IIR filters as opposed to FIR filters for orthogonal wavelets. This wavelet does not satisfy the admissibility condition.

8. **Mexican hat wavelet**: This wavelet is proportional to the second derivative of the Gaussian probability density function. It has infinite support width, but its effective region is the closed interval [-5,5]. This wavelet is also usually implemented using IIR filters.

9. **Gaussian Derivatives**: This wavelet family is given by the p^{th} derivative of the Gaussian function.
$$\psi(t) = C_p e^{-t^2}$$
where C_p is such that norm of the p^{th} derivative is 1.

10. **Complex Gaussian wavelets**: This wavelet family is given by the p^{th} derivative of the complex Gaussian function
$$\psi(t) = C_p e^{-it} e^{-t^2}$$
where C_p is such that norm of the p^{th} derivative is unity.

3 MATERIAL IDENTIFICATION METHODS USING CWT

The methods for material identification based on the continuous wavelet transform have been discussed in this section.

3.1 THE PROBLEM OF MATERIAL CLASSIFICATION

In general, the steps for material identification data acquisition (signal measurement), preprocessing, feature extraction and classification, [5]. Each of these have been discussed below.

3.1.1 Signal Measurement. For THz signal measurements, two of the common methods are to get the data through the THz-TDS or Fourier transform spectroscopy, [18]. The data used here have been based on the THz-TDS. THz-TDS offers the additional advantage of providing the phase information along with the amplitude information, which is not possible in the Fourier transform based techniques like FTIR, [2]. FTS based detectors measure power instead of electric field and lack the phase information. An additional advantage of TDS is that the power level for TDS are higher than those available with FTS, [18]. The additional phase information that is available in the TDS has been exploited in the wavelet transform methods for material identification.

3.1.2 Preprocessing. Measurement of the signals in the real world brings in artifacts like the effects of measuring system characteristics and noise. The combined effect of these two is the addition of noise to the convolution of the desired sample signals with the system transfer function. The goal of preprocessing is to remove the effect of noise and the system characteristics. The methods used to get the original signal have been noise removal followed by deconvolution. The noise removal methods that could be employed for noise removal are filtering, wavelet-denoising, etc. Deconvolution usually involves dividing the spectra of the sample signal by the spectra of the reference signal, [5]. However, the process of deconvolution is extremely sensitive to noise and can result in undesirable features that might lead into misleading features in the feature extraction stage.

3.1.3 Feature Extraction. One of the most common approaches for feature extraction has been the use of absorbance peaks (material absorption). The material absorption (α) is given by the following expression [4]

$$\alpha = -\frac{2}{d}\ln\left(\frac{E_{\text{signal}}(v)}{E_{\text{reference}}(v)}\right)$$

where d is the thickness of the pellet and $E_{\text{signal}}(v)$ and $E_{\text{reference}}(v)$ are the signal and reference frequency domain amplitudes, respectively.

The absorption spectra obtained by the above method results in a spectrum specific to the material, with peaks and valleys. In the terahertz range, each material tends to absorb a particular range of frequencies that cause the phonon resonance in the material, which in turn is attributed to the crystal structure of the material. This results in peaks in the absorption spectra at those specific frequencies, that provide a signature of the material. A signal with remnant noise in either of the reference material or the measured signal with test material can result in false peaks in the absorption spectrum. Sometimes Wiener filters are used to overcome this problem.

Shen et al. in [3] has used the refractive index for the identification of the RDX. They also showed that the first derivative of the spectrum measured in reflection mode is the same as that measured in transmission mode. One more feature that has been suggested is a parameter similar to absorption coefficient that is calculated based on the use of the wide-band cross ambiguity function defined as

$$\text{WBCAF}_{x_1}x_2(\tau,\sigma) = \frac{1}{\sqrt{\sigma}}\int_{-\infty}^{\infty} x_2(t)x_1^*\left(\frac{t-\tau}{\sigma}\right)\,\mathrm{d}t \qquad \forall\sigma,\tau\in R \tag{3.1}$$

where $x_1(t)$ is the reference waveform and $x_2(t)$ is the attenuated sample waveform. The absorption parameter in this approach has been defined as $\frac{\max_\tau(\text{WBCAF}_{\text{f}_1}\,\text{f}_2[\tau,\sigma])}{\max_\tau(\text{WBCAF}_{\text{f}_1}\,\text{f}_1[\tau,\sigma])}$ This ratio corresponds to a measure of relative transmission and hence can be used as a measure similar to absorption coefficient.

3.1.4 Classification. Various classification schemes like Mahalanobis distance, K-Nearest Neighbor, Nearest Mean, Neural Networks, Correlation Coefficients etc. can be used for classification purposes.

The above mentioned methods describe how the material classification has been dealt. Next, the methods used for the material detection in this thesis work will be discussed.

3.2 COMMON STEPS FOR ALL THE CWT BASED METHODS

Following are the steps common to all the four methods for material identification based on continuous wavelet transform discussed in this section.

Step 1: Determine the CWT coefficients for the test signal. The continuous wavelet transform coefficients for the test signal are calculated using the Equation (2.3). The parameters to be chosen are the wavelet for analysis and range of scales to cover the complete signal over the length of time it persists. The result is a 3-dimensional surface with scales and shifts as the variable. Such a 3-dimensional surface for the continuous wavelet transform coefficients calculated using one of Daubechies wavelets is shown in Figure 3.1.

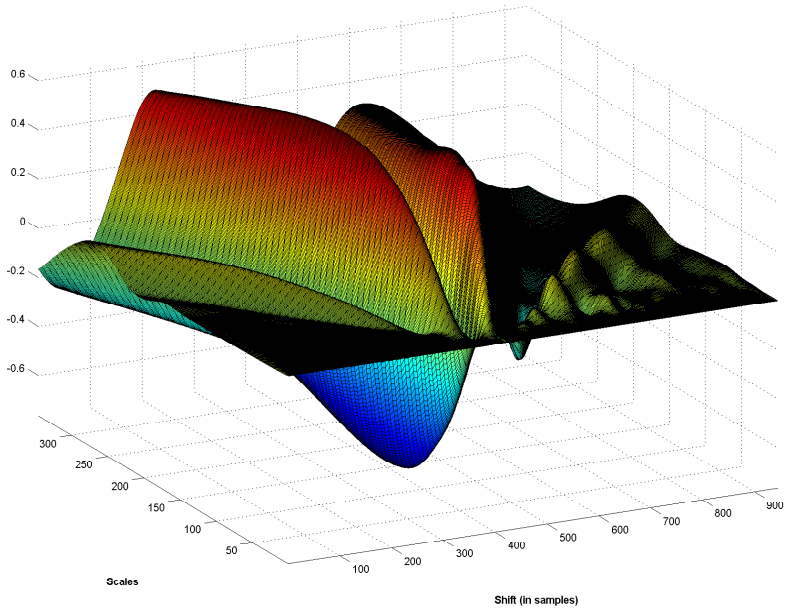

Figure 3.1. Continuous wavelet transform coefficients using Daubechies wavelet of order 6 and scales from 1 to 350.

Step 2: Determine the energy density in the time scale domain for the signal using the CWT coefficients. Equation (2.9) is used to calculate the energy density in the time scale domain. This step can be accomplished by dividing all the coefficients by their respective scales squared. The results of this is a smoother surface decaying faster than the CWT surface because of the normalization by large values of scales towards high scale region. One such surface for the signal is shown in Figure 3.2.

Step 3: Remove the noisy portion of the time energy density by determining the partial derivatives along the scales. The partial derivative of the CWT function is calculated. The values of function at small scales (corresponding to high frequencies) usually have very high values due to noisy nature of the signal. As a result, the coefficients' amplitude varies widely at small scales. One scheme to remove these noisy components is to calculate the values of derivatives along the direction of shifts and retain only those coefficients that correspond to a derivative

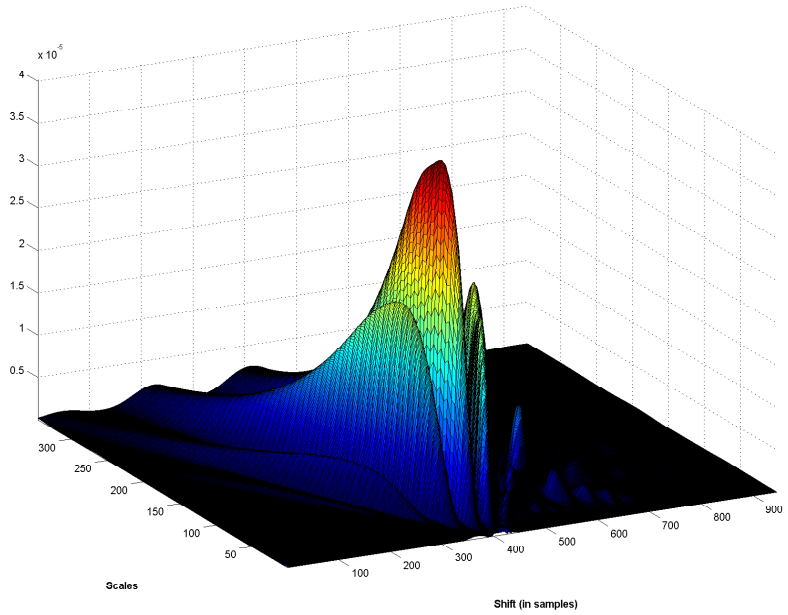

Figure 3.2. Energy density in the time scale domain for time signal using Daubechies wavelet of order 6 and scales from 1 to 350.

smaller than a threshold. This threshold is chosen as the maximum value of the derivative found out for a noiseless signal. This step is similar to the preprocessing stage in Section 2.

Step 4: Find out the maxima lines using the energy density coefficients. This step is accomplished by finding the local maxima in a neighborhood (decided by the chosen frames size) for a particular scale. Time energy density coefficients that correspond to an energy level less than 5% of the peak energy are discarded to overcome the effect of noise and utilize only the high energy portion of the signal for identification. The same procedure is repeated for all the scales. The collection of such maxima points will serve as the maxima lines. Figure 3.3 shows the maxima lines for one of the test signals.

Step 5: Find out the ridge lines (ridges) using the energy density coefficients. This step is accomplished by finding the local maxima in a neighborhood (decided by the frames size chosen) for a particular shift rather than scale as in Step 4. Time-energy density coefficients which correspond to an energy level less than 5% of the peak energy are discarded to overcome the effect of noise and utilize only the high energy portion of the signal for identification. The same procedure is repeated for all the shifts. The collection of such maxima points will serve as the ridge lines. Figure 3.4 shows the ridge lines for one of the test signals.

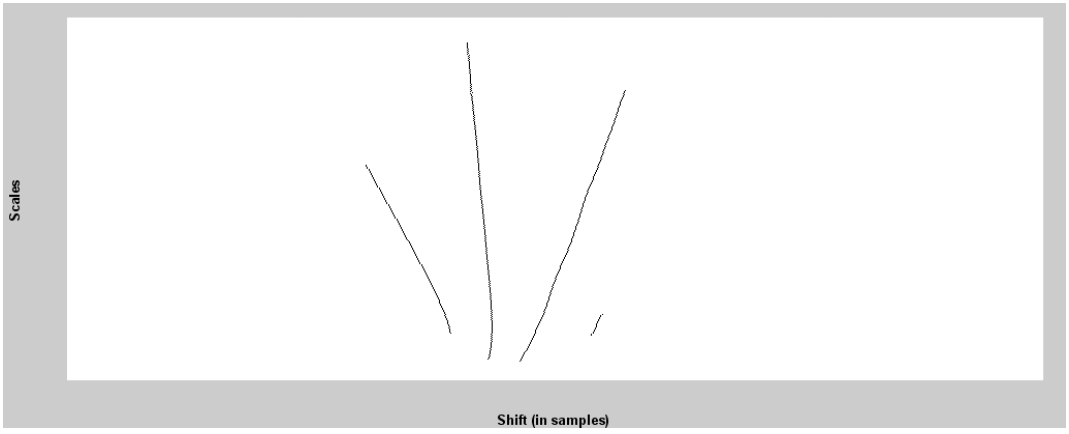

Figure 3.3. Maxima lines for the time-energy density coefficients for a sample time signal using Daubechies wavelet of order 3 and scales from 1 to 350.

After going through the above steps, one of the following four methods can be used for the stage purpose of material identification.

3.2.1 Combination of Maxima Lines and Ridges with Shift. The maxima lines and ridges found out in Steps 4 and 5 above are sufficient to be used as features for the material identification. The coordinates of these two features can be used to create binary images. A measure of the correlation between the test binary image and similar images that are available off-line can be done. This would give a measure of the correlation between the two images that could be compared against a pre-decided threshold value to serve as a match indicator. This method does not take into account the shift that the test signal might have undergone. Thus, it assumes that both the absolute and the relative location of peaks are important for the signal determination. Figure 3.5 shows the combined maxima lines and ridges obtained by combining data points from Steps 4 and 5.

3.2.2 Combination of Maxima Lines and Ridges without Shift. This method of identification considers the shift of the signal in the time domain. Thus, it addresses the issue that the test signals obtained through signal measurement techniques might be time shifted versions of the signal present in the library of signals. Effectively, it reduces the burden of storing time-shifted versions of the signal in the library. For finding the coefficient of correlation, the binary images are moved along

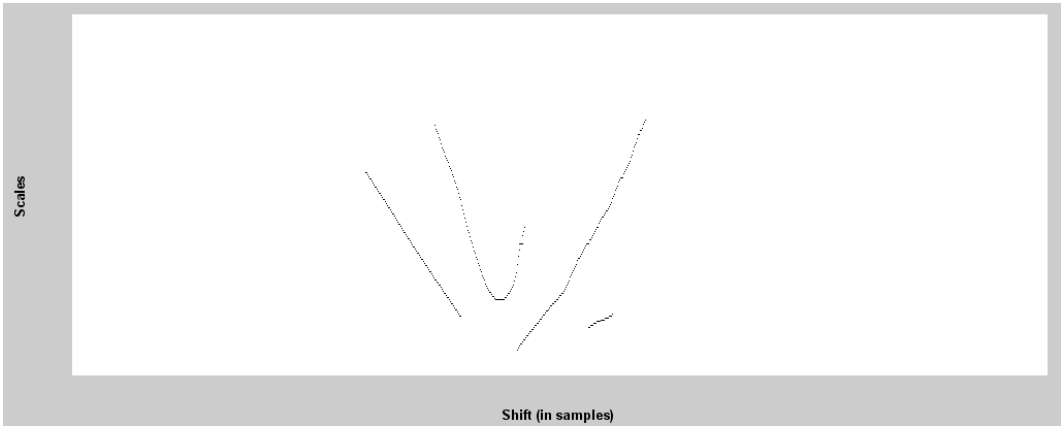

Figure 3.4. Ridge lines (ridges) for the time-energy density coefficients for a sample time signal using Daubechies wavelet of order 3 and scales from 1 to 350.

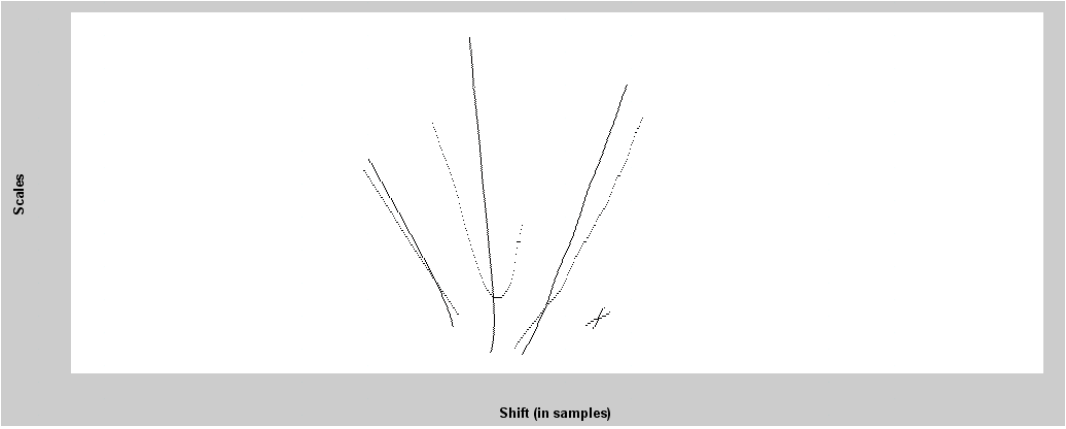

Figure 3.5. Maxima lines and ridges combined for the time-energy density coefficients for a sample time signal using Daubechies wavelet of order 3 and scales from 1 to 350.

the shift axis giving a sequence of correlation coefficients for all the shifts. The maximum value of the correlation coefficient is then chosen to be compared with the threshold value. This method assumes that only the relative location of peaks are important for the signal determination, but not the absolute locations.

3.2.3 Intersection Points with Weights with Shift. Instead of using all the set of points obtained using maxima lines and ridges as features, only their points of intersection can be treated as classifying features as well. This can be accomplished by assigning weights to these points by using a geometric shape with area proportional to the energy levels at those points that are calculated already in Step 2. Then their correlation (without shifting) with the same features of the previously computed library materials can be determined. This method assumes that both the absolute and the relative location of intersection points are important for the signal identification. Figure 3.6 shows the intersection point locations for a sample time signal.

3.2.4 Intersection Points with Weights without Shift. This method is similar to the previous method, but with the shift taken into account. As in Section 3.2.3, for finding the coefficient of correlation, the binary images are moved along the shift axis giving a sequence of correlation coefficients for all the shifts. The maximum

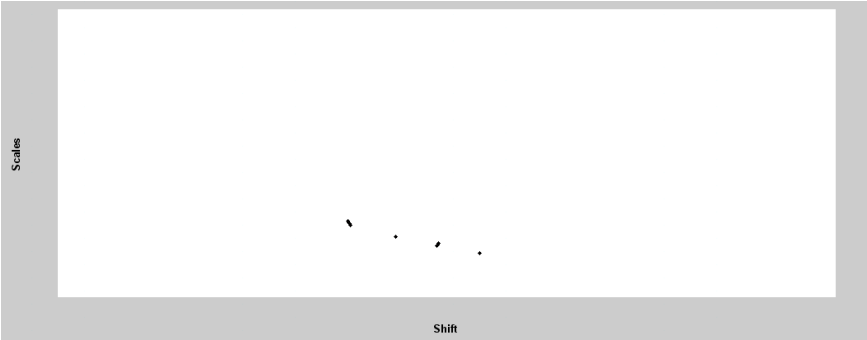

Figure 3.6. Intersection points of maxima lines and ridges for time-energy density coefficients for a sample time signal.

value of the correlation coefficient is then chosen to be compared to the threshold value. This method assumes that only the relative location of points of intersection is important for the signal determination, but not the absolute locations.

The implementation of these methods and the results obtained are discussed in Section 5.

4 MATERIAL IDENTIFICATION METHODS USING DWT

The methods of material identification used earlier as well as the proposed method based on the discrete wavelet transform have been discussed in this section. Since the discrete wavelet transform is inherently shift variant, no methods based on shifting properties have been discussed.

4.1 EARLIER EFFORTS FOR IDENTIFICATION USING DWT

The discrete wavelet transform had been used earlier mainly for the purpose of de-noising the signals. Efforts have been done to de-noise the signals using the process of soft-thresholding in [10] and [5]. This method involves the use of filter-banks in a recursive manner to calculate the discrete wavelet transform coefficients and particularly suitable for non-stationary pulse like signals.

In soft-thresholding, the sample variance of the coefficients in a band is calculated and the threshold is set to some multiple of the standard deviation. The wavelet coefficients are suppressed to zero if their values are below the threshold or left unaltered otherwise, [13]. The result of this processing is that small energy coefficients representing noise are filtered out while the coefficients greater than or equal to the threshold, which in fact represent the high energy content portion of the signal, are retained.

Handley et al. in [5] had used the discrete wavelet transform to find optimal wavelets through experimentation. Noise was added to the original signals and a de-noising algorithm applied using different wavelets. The criterion for choosing the optimal wavelet was based on obtaining the best signal to noise ratio (SNR) after the application of the set of wavelets.

Shopov et al. in [12] had used the ultrasonic echo signal returned after reflection from the target explosive material for explosive material classification. This method involved processing the reflected signal using the discrete wavelet transform to decompose the signals to level 7 and 8 and use the approximation coefficients as the recognition attributes (features). The system was trained using multiple data sets and classified using the K-nearest neighbor classification scheme.

4.2 PROPOSED DWT METHOD

The test data used for testing this method is the same as the data used earlier in the CWT methods. As described in Section 2, the signal can be divided into sub bands using the orthogonal DWT by continuous filtering and down-sampling. Each step of filtering and down-sampling through a pair of low-pass and high-pass filters results in two sub-sequences corresponding to the lower and higher frequency band, each with dimensions approximately half of the original signal. The size of the filtered sequence depends on the size of the filter chosen, which in turn depends on the wavelet chosen for analysis. Each of the resultant sub-sequences is then further passed through the same procedure. If the process is continued k many times, the original signal is decomposed to level k and the result is a set of 2^k sub-band sequences of equal bandwidths and dimensions reduced by a factor of 2^k. The lowest sub-band comprises of the frequencies starting from DC to $(\pi/2^k)$. The next higher band is of the same bandwidth but starting from the higher cut-off frequency of the upper band and so on.

Naturally, these sub-bands are of equal size since they are at the same level of decomposition. Denoting L as the length of the sequence at level k, these sub-bands are placed parallel to each other resulting in a matrix of dimension 2^k by L. The absolute values of these sequences are placed in increasing order of their frequency contents, so that the first corresponds to the lowest sub-band and the last row to highest sub-band. This arrangement is similar in a sense to the CWT matrix in Section 3, but a linear increase in scaling factor is substituted by a grouping of scale ranges. Thus, this new matrix arrangement has sub-bands along one axis and the corresponding sequence index along the other. The third dimension is the absolute value of the DWT coefficient, which is a measure of the energy content in that particular band.

4.3 COMMON STEPS FOR ALL THE DWT BASED METHODS

The steps common to all the four methods for material identification based on the discrete wavelet transforms discussed in this section are given below.

Step 1: Determine the discrete wavelet transform coefficients using filter-banks to a fixed level of decomposition. The discrete wavelet transform

coefficients for the test signal are calculated using the filter-banks through iteratively filtering the sub-bands for a given level (k) of decomposition until 2^k sub-band sequences are obtained. The set of filter-banks is dependent on the orthogonal wavelet chosen for analysis.

Step 2: Arrange the sub-band sequences to form a 2-dimensional matrix. As mentioned in the previous section, the sub-bands are arranged to form a matrix. Absolute values of the coefficients are then used for further operations. The surface formed by such a matrix is shown in Figure 4.1. Once the matrix is obtained, one of the following algorithms can be used for the identification.

4.3.1 Maxima Lines/Points. The maxima lines in the context of discrete wavelet transform can be redefined as a function of sub-band number and the index of the coefficient in the sub-band instead of the shift and the scale variables. This is in a way similar to the continuous wavelet transform method because choosing a particular sub-band is equivalent to choosing a range of scales; but in a non-redundant way. The maxima lines/points are found for the test and the library materials and then converted to corresponding binary images. The correlation between the corresponding binary images is then computed. The material yielding the coefficient of correlation greater than a pre-decided threshold value with the test material is then declared as the target material. A binary image showing the maxima points obtained for

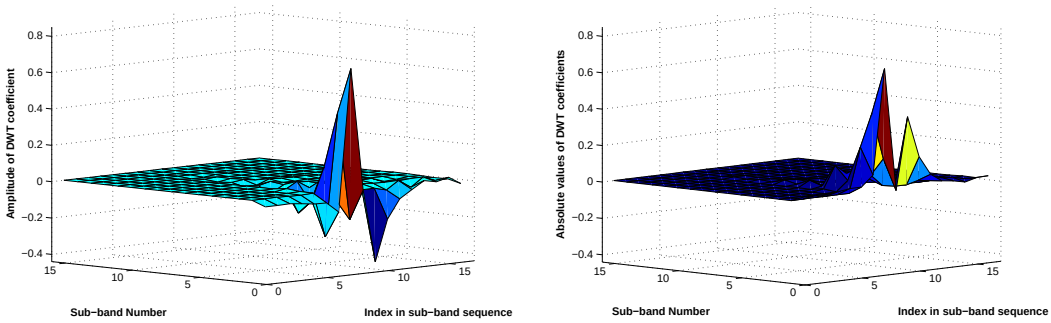

(a) Actual values (b) Absolute values

Figure 4.1. Sub-band sequences arranged in matrix form.

a library signal is given in Figure 4.2. The orthogonality of the discrete wavelet transform results in a minimum number of coefficients, which makes it difficult to have continuity of points like the one obtained in continuous wavelet transform methods.

4.3.2 Ridge Lines/Points. This method is the same as identification using maxima lines except that ridges instead of maxima lines are used for identification purpose. A binary image showing the ridge points obtained for a library signal is given in Figure 4.2.

4.3.3 Combination of Maxima Lines and Ridge Lines. This method combines the pixels identified by both the maxima points and the ridges and uses the combined features for identification. A binary image showing the maxima points and ridge points obtained for a library signal is given in Figure 4.3.

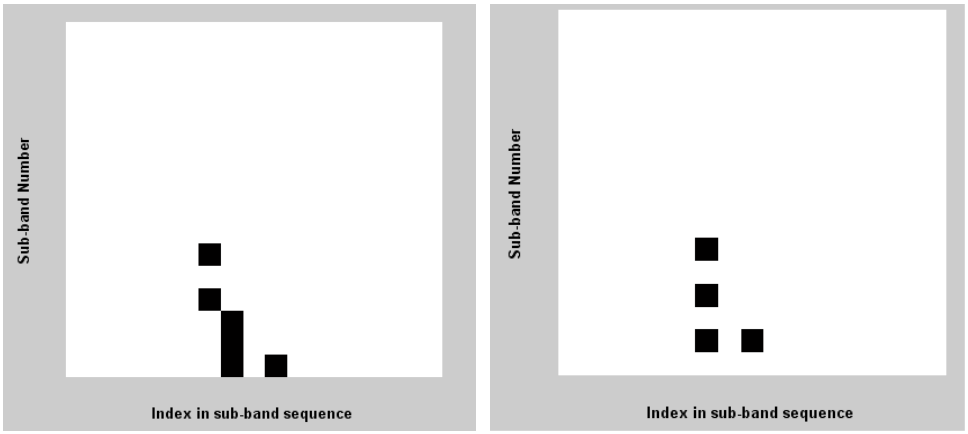

(a) Maxima points (b) Ridge points

Figure 4.2. Binary image for maxima and ridge points using sub-band sequences obtained through DWT.

4.3.4 Intersection Points of the Maxima Lines and Ridges. This method uses the intersection points of the maxima lines and the ridges as features for identification. A binary image showing the intersection of maxima points and ridge points obtained for a library signal is given in Figure 4.3.

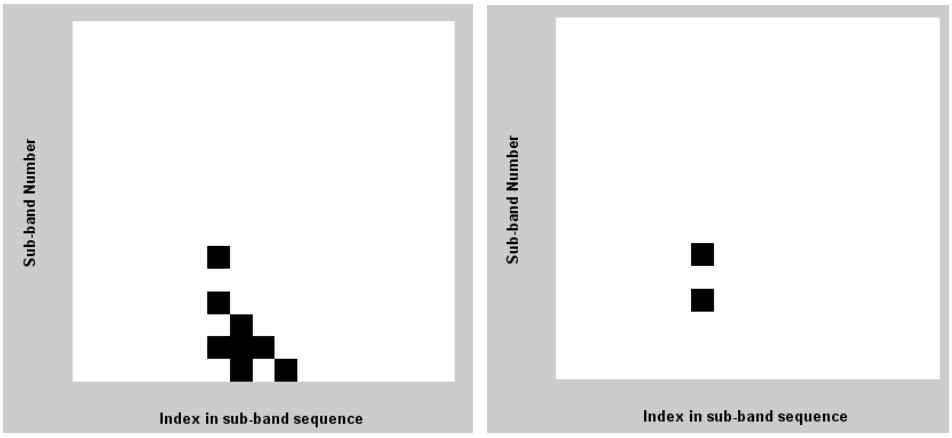

(a) Maxima points and ridge points combined.

(b) Intersection of maxima points and ridge points combined.

Figure 4.3. Binary image for maxima points and ridge points combined and their intersection points using sub-band sequences obtained through the DWT.

The implementation of these methods will be discussed in Section 5.

5 TARGET MATERIAL DETECTION USING WAVELET TRANSFORM

In this section, the application of the methods described in Sections 3 and 4 as applied to signals obtained through the terahertz time-domain spectroscopy have been discussed. The suitability and the robustness of each of the methods has been tested under different noise conditions (i.e. different signal to noise ratios) with different wavelets. Criteria for choosing wavelets that best classify the test data available have also been suggested.

5.1 TEST DATA

The test data has been obtained from the same source that was used in [4]. The signals consisted of 945 samples for each of the materials HMX, PETN, RDX and TNT, where the material descriptions are discussed in the Appendix. The sampling rate for the signals was 75 tera-samples per second. The data was obtained using the THz-TDS obtained in transmission mode. The target materials were crystallized from solvent form, followed by drying, weighing, and grounding. The grounded material was then pressed into pellets with a polyethylene (PE) binder with 3.5–4.5 micrometers mean particle size.

The methods described in Sections 3 and 4 have been tested by adding different levels of white Gaussian noise to the pure target materials. Figure 5.1 shows a pure terahertz signal and the same signal with additive noise.

To give an idea to the reader of the effect of noise of various levels, 100 of noise added signals with a specific noise level have been added on the top of each other along with the original signal in Figure 5.2.

5.2 RESULTS FOR CWT METHODS APPLIED TO TEST DATA

The data source claims that the useful range of frequencies is upto 6 THz. This implies a useful range of scales starting at 12.5 (=75THz/6THz) and beyond from the perspective of the CWT. It turns out that the number of peaks generated by a particular wavelet depends on the number of maxima and minima in the signal, as

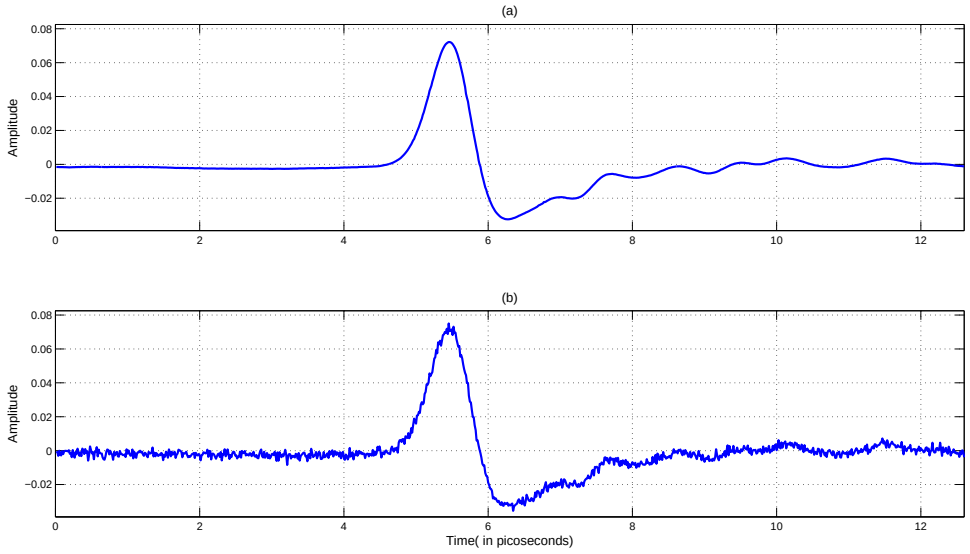

Figure 5.1. Pure and noise added time domain signals obtained through terahertz time-domain spectroscopy.

well as the regularity of the wavelet. The more regular a wavelet is, the more number of times it oscillates up and down within its support width. Thus, increasing the order of the wavelet results in the increase in the number of peaks and correspondingly the number of maxima lines and the intersection points.

All the steps (1 though 5) described in Section 3 were carried out in sequence, resulting in preprocessed coefficients available for feature determination. Figures 5.3 and 5.4 show the CWT function values before and after the noise removal, respectively. The effect of the noise removal process is clearly visible.

5.2.1 Using Maxima Lines and Ridges with Shift. Once the above steps have been carried out, the correlation of the test image is carried out with the library materials with the lateral shift and the maximum of the correlation coefficient. The reason both the maxima lines and the ridges have been used in this method is because for the set of test data, both the ridges and maxima lines are different and provide unique features.

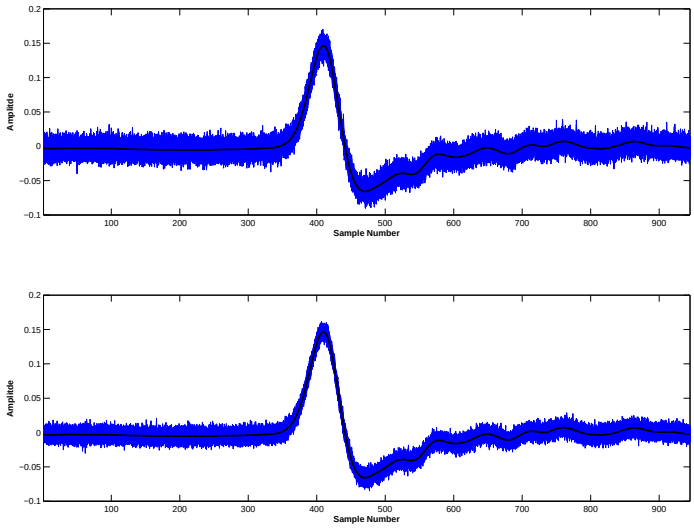

Figure 5.2. Time domain signals with the band created by a number of noise signals of SNR 12dB and 15dB added to pure HMX signal.

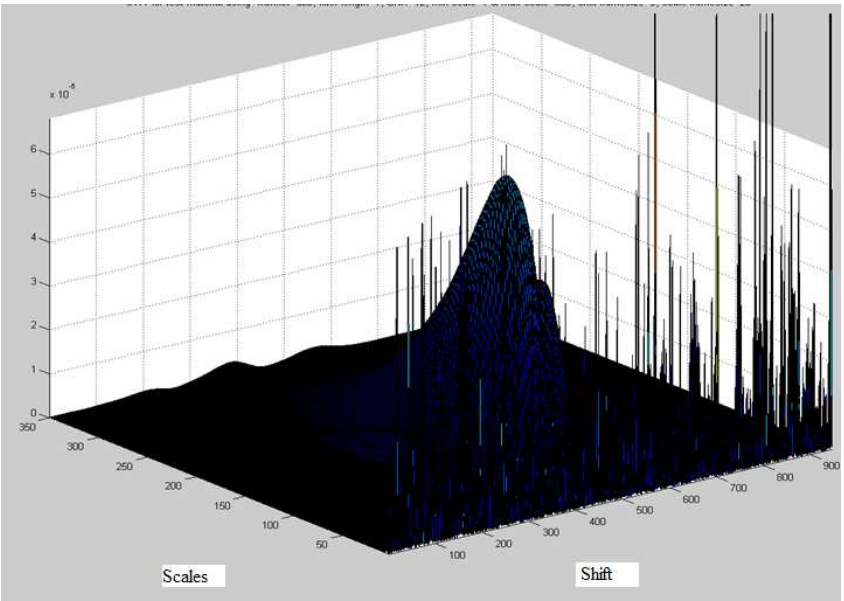

Figure 5.3. Time energy density coefficients with SNR 12dB before noise removal.

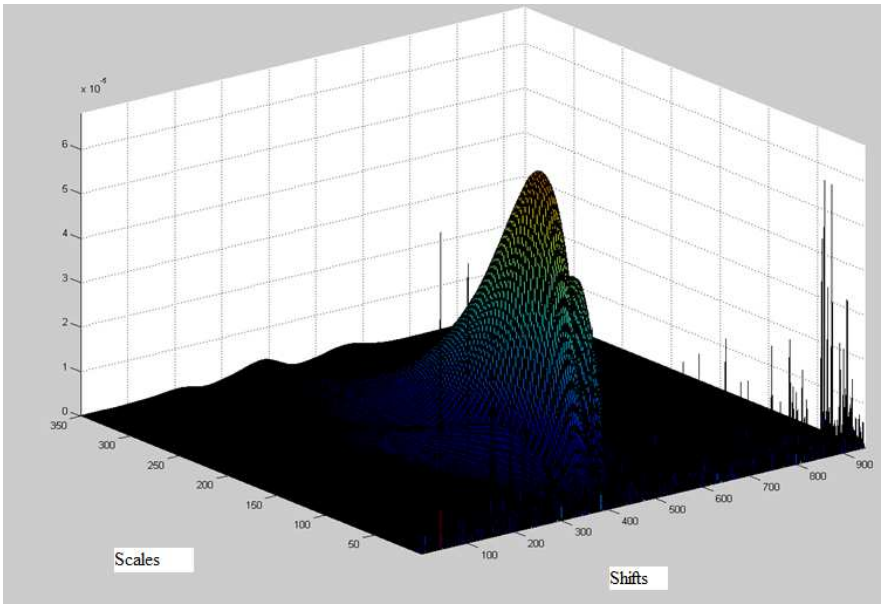

Figure 5.4. Time energy density coefficients with SNR 12dB after noise removal.

The method was tested for different levels of signal to noise ratio using additive white Gaussian noise. Table 5.1 shows the results for such simulations for 50 different cycles of same noise level corresponding to the four materials in the library.

5.2.2 Using Maxima Lines and Ridges without Shift. The method is similar to the previous method without the signal shift. This method gives better results than the above method with shift and was able to identify the materials with a threshold set to 0.5. Figure 5.5 shows the confusion matrix represented as a 3-dimensional bar graph for the four test materials with an SNR of 12dB as well as an additional signal. The confusion matrix here represents a degree of correlation among the different materials. So, a test material obtained by adding noise to a pure material will show a higher correlation against the pure material, than against the other library materials. The brown bars represent the correlation coefficient of the test material against the materials in the library. Clearly, the test material has very low correlation against all the library materials (less than the decided threshold of 0.5).

Table 5.1. Detection accuracy using maxima lines and ridges with shift for the library materials using wavelet db10.

Test Material	**Signal to noise ratio in dB**	**Percentage accuracy**	**Minimum coefficient of correlation**
HMX	14	4	0.37
HMX	15	80	0.45
HMX	16	88	0.47
HMX	17	100	0.52
PETN	14	6	0.37
PETN	15	36	0.38
PETN	16	70	0.47
PETN	17	98	0.49
PETN	18	100	0.53
RDX	14	2	0.35
RDX	15	12	0.40
RDX	16	66	0.45
RDX	17	92	0.47
RDX	18	100	0.53
TNT	14	0	0.35
TNT	15	24	0.37
TNT	16	84	0.43
TNT	17	100	0.51

The innermost orange bar in second row represents the correlation between the material 4 (TNT) with and without noise. This bar is higher than the correlation coefficient bars against other library materials (the other 3 orange bars). Similarly, RDX (material 3), PETN (material 2) and HMX (material 1) have the highest correlation coefficient at the diagonals, showing highest correlation of the noise added material with the pure material rather than with any other library material.

The method was tested for different levels of signal to noise ratios using additive white Gaussian noise. Table 5.2 shows the results for such simulations for 50 different cycles of the same noise level corresponding to the four materials in the library. As evident from the table, the detection accuracy increases with better signal to noise ratio.

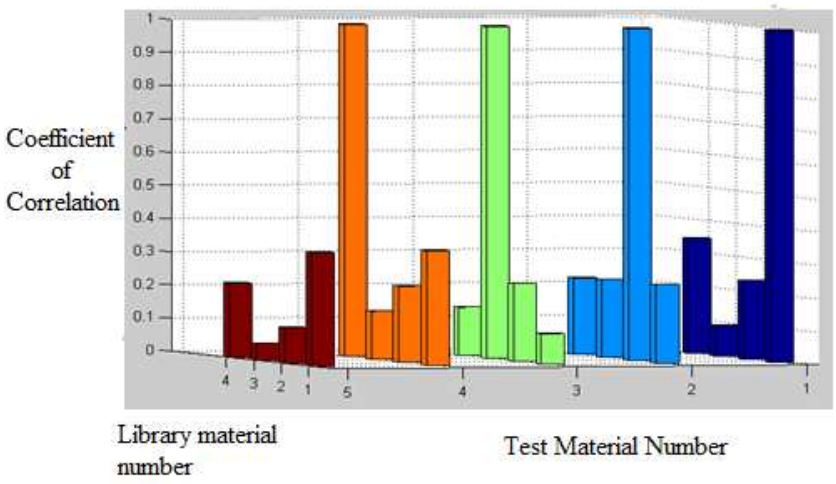

Figure 5.5. Correlation coefficients with library materials and a non-library material.

5.2.3 Using Intersection Points with Weights with Shift. In this method, a weight (effectively an area in a binary image with a geometric shape) is assigned to the intersection points. The shape chosen is similar to the *plus* symbol with the area of the shape proportional to the time-energy density coefficient. This ensures that high energy coefficients are given more importance over others. Figure 5.6 shows such a weight allocation scheme.

A better way to decide the geometric shape is to add noise to the pure signal and look for the displacement of the intersection points for a number of test signals. One such simulation for 100 noisy signals with 20dB noise is shown in Figure 5.7. Clearly, the exact geometric shape requires an intricate shape customized for each point. Implementation of such shapes would greatly increase the accuracy of the identification.

The method was tested for different levels of signal to noise ratio using additive white Gaussian noise. Table 5.3 shows the results for such simulations for 50 different cycles of the same noise level corresponding to the four materials in the library.

Table 5.2. Detection accuracy using maxima lines and ridges without shift for the library materials using wavelet db10.

Test Material	Signal to noise ratio in dB	Percentage accuracy	Minimum coefficient of correlation
HMX	14	46	0.37
HMX	15	46	0.43
HMX	16	86	0.45
HMX	17	100	0.52
PETN	14	0	0.39
PETN	15	22	0.42
PETN	16	78	0.46
PETN	17	94	0.47
PETN	18	100	0.52
RDX	14	2	0.38
RDX	15	10	0.42
RDX	16	68	0.45
RDX	16	94	0.49
RDX	17	100	0.52
TNT	14	2	0.35
TNT	15	28	0.39
TNT	16	88	0.48
TNT	17	100	0.51

5.2.4 Using Intersection Points with Weights without Shift. This method is similar to the previous method, but without shift. The method was tested for different levels of signal to noise ratio using additive white Gaussian noise. Table 5.4 shows the results for such simulations for 50 different cycles of same noise level corresponding to the four materials in the library.

5.3 RESULTS FOR DWT METHODS APPLIED TO TEST DATA

For testing the methods using the DWT, similar methods were employed for adding noise to the pure signal and then testing them against the library signals. One important point to be noted is that the DWT is shift invariant by nature, which means that the correlation by shifting the binary images cannot be determined. The signals were decomposed to level 6 ($k = 6$), giving a total of 64 sub-band sequences.

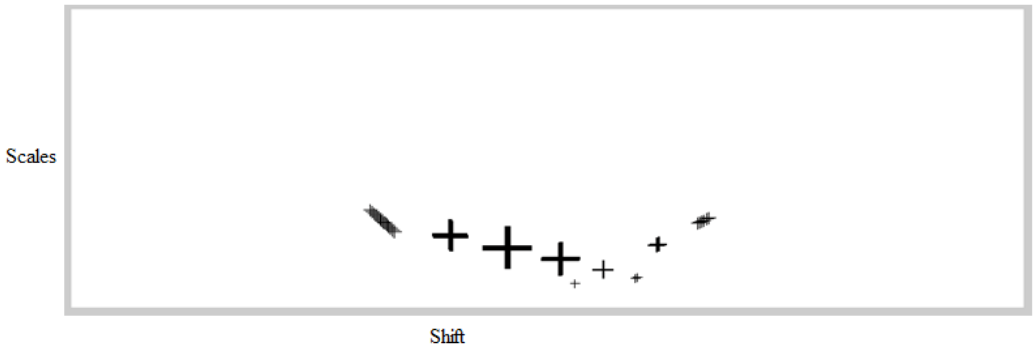

Figure 5.6. Figure showing weights assigned to the intersection points of maxima lines and ridges.

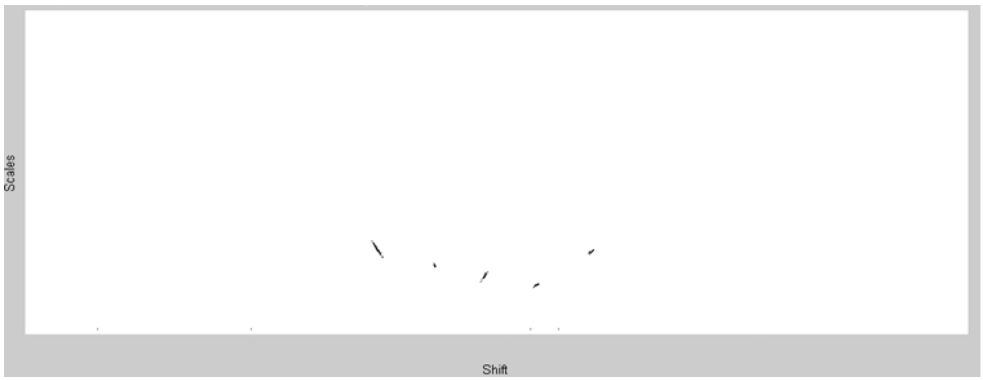

Figure 5.7. Movement of intersection points with 20dB noise.

The reason for decomposing the signals to such a high level is that the available test signals are narrow-band signals and only the lowest sub-bands have the majority of the energy content of the signal. This property was verified from the amplitude spectrum (FT) of the signals. To be able to observe some variation across the sub-bands, the signal needs to be decomposed into more levels so that the energy at the lower frequency sub-bands correspondingly separated.

5.3.1 Using Maxima Lines Alone. The methods suggested in Section 4.3.1 were tested by adding different levels of noise to the pure signals. To a smaller degree, the addition of noise resulted in some level of energy being transferred to

Table 5.3. Detection accuracy using intersection of maxima lines and ridges with weights (with shift) for the library materials using wavelet db3.

Test Material	**Signal to noise ratio in dB**	**Percentage accuracy**	**Minimum coefficient of correlation**
HMX	12	78	0.29
HMX	13	90	0.39
HMX	14	96	0.33
HMX	15	98	0.44
HMX	16	100	0.54
PETN	12	76	0.27
PETN	13	92	0.26
PETN	14	96	0.42
PETN	15	100	0.52
RDX	12	68	0.30
RDX	13	82	0.31
RDX	14	86	0.35
RDX	15	94	0.37
RDX	16	100	0.51
TNT	12	70	0.32
TNT	13	86	0.28
TNT	14	94	0.33
TNT	15	98	0.46
TNT	16	100	0.50

the higher sub-bands as well. Only the lower 16 sub-bands were retained because the higher bands still did not have appreciable energies. This also serves to reduce the computational load for narrow-band signal. The maxima points were then found out and the correlation coefficients are determined. Figure 5.8 shows the confusion matrix similar to the ones mentioned in the previous sections with all the four noisy signals serving as test signals.

The method was tested for different levels of signal to noise ratio using additive white Gaussian noise. Table 5.5 shows the results for such simulations for 50 different cycles of same noise level corresponding to the four materials in the library using wavelet *db*2 (Daubechies wavelet of order 2).

Table 5.4. Detection accuracy using maxima lines and ridges with shift for the library materials with wavelet db3.

Test Material	**Signal to noise ratio in dB**	**Percentage accuracy**	**Minimum coefficient of correlation**
HMX	14	84	0.34
HMX	15	88	0.45
HMX	16	92	0.48
HMX	17	98	0.44
HMX	18	98	0.45
HMX	19	100	0.52
PETN	13	74	0.25
PETN	14	94	0.42
PETN	15	92	0.47
PETN	16	96	0.47
PETN	17	100	0.52
RDX	14	64	0.31
RDX	15	86	0.37
RDX	16	88	0.42
RDX	17	98	0.47
RDX	18	96	0.39
RDX	19	96	0.45
TNT	14	88	0.43
TNT	15	100	0.55
TNT	16	98	0.38
TNT	17	94	0.42
TNT	18	100	0.53

5.3.2 Using Ridges Alone. The methods suggested in Section 4.3.2 were tested by adding different levels of noise to the pure signals and procedure similar to the one followed for maxima points carried out. However, the number of points obtained were fewer than those for maxima points. Figure 5.9 shows the confusion matrix with all the four signals added with noise and serving as test signals.

The method was tested for different levels of signal to noise ratio using additive white Gaussian noise. Table 5.6 shows the results for such simulations for 50 different cycles of same noise level corresponding to the four materials in the library using wavelet *db*2 (Daubechies wavelet of order 2).

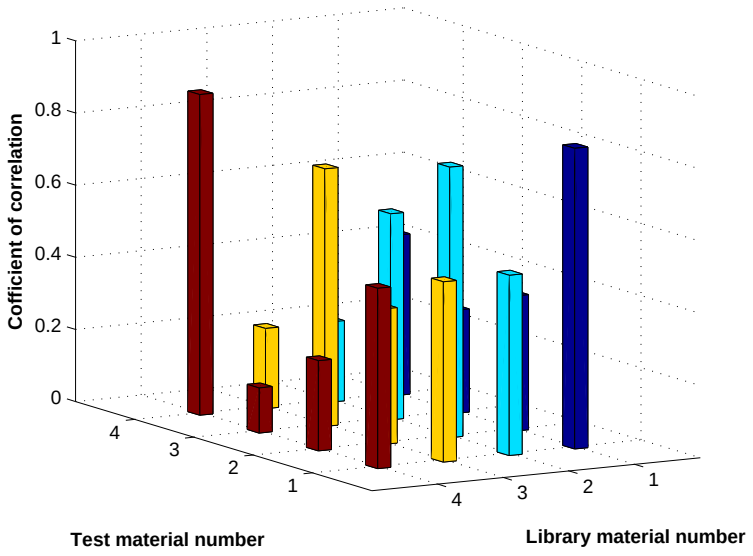

Figure 5.8. Confusion matrix shown as a 3-dimensional bar plot using maxima points and SNR 15dB using Daubechies order 2 wavelet.

5.3.3 Using Combination of Maxima Lines and Ridges. The methods suggested in Section 4.3.3 were tested by adding different levels of noise to the pure signals and a procedure similar to the one followed for maxima points and ridge points was followed. Figure 5.10 shows the confusion matrix with all the four signals having been added with noise and serving as test signals. Table 5.7 shows the results for such simulations for 50 different cycles of same noise level corresponding to the four materials in the library using wavelet db2 (Daubechies wavelet of order 2).

5.3.4 Using Intersection of Maxima Lines and Ridges. Since the points of intersection are too few, this might not be a very reliable method. Weights similar to the ones used in the CWT methods can't be used because the corresponding rows are from completely different bands, unlike consecutive scales which are correlated to each other to some extent.

5.4 CHOICE OF WAVELETS

The wavelets chosen for analysis play an important role for the purpose of feature identification using both the CWT and the DWT methods. The regularity of

Table 5.5. Detection accuracy using maxima lines alone for the library materials.

Test Material	**Signal to noise ratio in dB**	**Percentage accuracy**	**Minimum coefficient of correlation**
HMX	9	40	0.29
HMX	10	54	0.31
HMX	11	76	0.44
HMX	12	90	0.40
HMX	13	100	0.56
PETN	9	98	0.43
PETN	10	96	0.38
PETN	11	98	0.45
PETN	12	100	0.50
PETN	13	100	0.60
RDX	9	86	0.30
RDX	10	94	0.38
RDX	11	96	0.40
RDX	12	100	0.50
RDX	13	98	0.43
RDX	14	100	0.50
TNT	9	48	0.32
TNT	10	72	0.31
TNT	11	100	0.50
TNT	12	100	0.60

a wavelet decides the number of ripples in the wavelet. The regularity of a wavelet increases with the order of the wavelet and gives more number of peaks in the 3-dimensional CWT function. The result is an increased number of maxima lines and ridges. This choice gives an increased number of features for classification, but at the same time increases the correlation coefficient because of the increased number of points in the binary image for overlapping.

The ideal wavelet should result in features that give correlation coefficient greater than the threshold for the desired material affected by noise, but less than the threshold for the other materials. The choice of threshold and corresponding wavelets depends on the type of signals and the degree of similarity between among the library materials. For the given test data, a threshold of 0.5 or lower worked

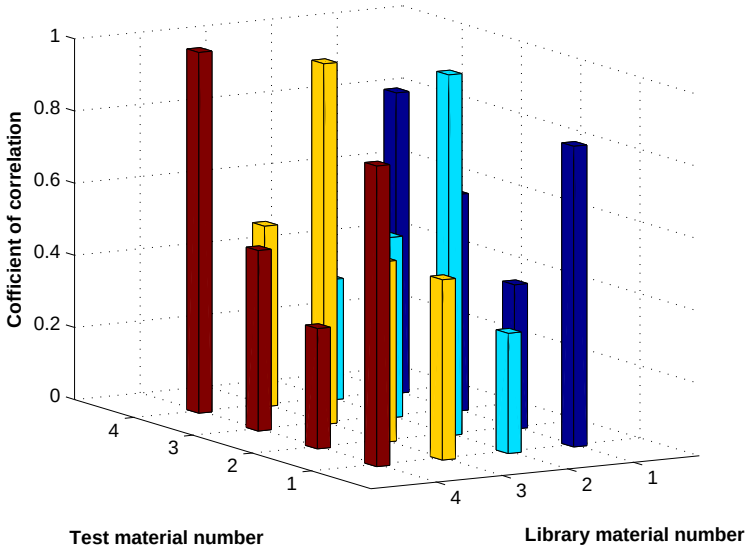

Figure 5.9. Confusion matrix shown as a 3-dimensional bar plot using ridge points and SNR 15dB using Daubechies order 2 wavelet.

well for the CWT based methods without shift with low false detections. For the shift invariant methods, a threshold of 0.5 was effective, but the false detections were higher. Lower false detections could be obtained by increasing the threshold for shift invariant methods. Table 5.8 shows the 100% accuracy of one of the CWT methods with different order of wavelets for HMX. As observed, higher order wavelets are able to classify the test signals better in presence of higher noise levels (lower signal to noise ratio). A disadvantage with the higher order wavelets is that the computational complexity increases with the increasing order of the wavelet.

For the DWT methods, the choice of wavelets determines the filter banks used. This decides the roll-off and band-widths of the low-pass and the high-pass filters, which in turn effects the sub-band sequences. Thus, different wavelets result in different features. Some wavelets tend to give better and unique features with the materials, which makes the classification process easy. Data obtained from different hardware would have different frequency components, and correspondingly work well with different wavelets.

Table 5.6. Detection accuracy using ridges alone for the library materials.

Test Material	Signal to noise ratio in dB	Percentage accuracy	Minimum coefficient of correlation
HMX	9	60	0.26
HMX	10	90	0.36
HMX	11	98	0.45
HMX	12	100	0.56
HMX	13	100	0.71
PETN	9	80	0.27
PETN	10	96	0.38
PETN	11	96	0.43
PETN	12	96	0.38
PETN	13	100	0.50
PETN	14	100	0.60
RDX	9	82	0.33
RDX	10	96	0.40
RDX	11	98	0.40
RDX	12	98	0.40
RDX	12	100	0.50
RDX	12	100	0.60
TNT	9	34	0.25
TNT	10	76	0.28
TNT	11	90	0.40
TNT	12	100	0.55
TNT	13	98	0.46
TNT	14	100	0.60

The best performance for the given data with the CWT methods was obtained by Daubechies wavelets of order 3 and 10 (db3 and db10). For the DWT based methods, the best performance was shown by Daubechies wavelet of order 2 and Symlet of order 10 (db2 and sym10).

5.5 COMPARISON WITH ABSORPTION SPECTROSCOPY

As mentioned in Section 2, the earlier methods used to rely on the peaks of the absorbance spectrum as identification features. A parallel cannot be drawn between the two methods because of the nature of the transforms. While absorption

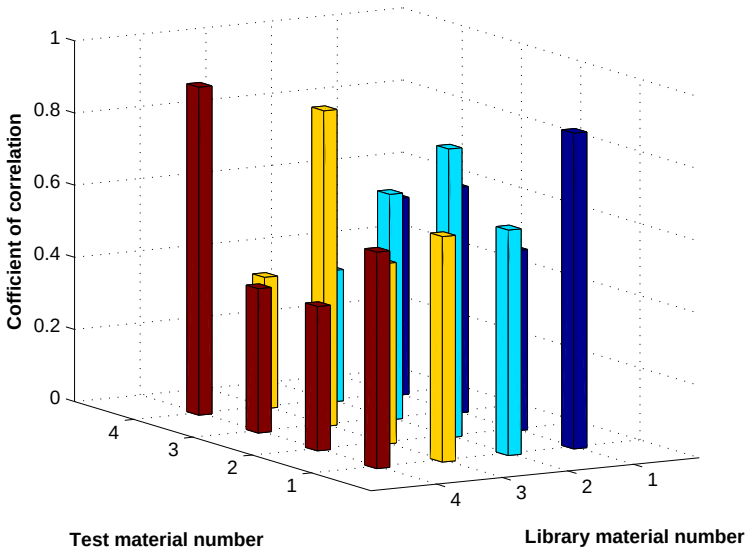

Figure 5.10. Confusion matrix shown as a 3-dimensional bar plot using both maxima and ridge points and SNR 15dB using Daubechies order 2 wavelet.

spectroscopy relies on the ratios of the Fourier transforms at different frequencies, the methods suggested in this thesis rely on the absolute values of the coefficients obtained through the continuous/disrete wavelet transforms. Each frequency in the absorption spectrum can be used as a candidate for the feature independent of the other one. But in the presented CWT based methods, the features have been obtained through maxima lines and ridges (locus of points rather than each point alone), which collectively act as a feature. For the DWT based methods too, the sub-band sequences correspond to a band of frequencies which can't be compared to the absorbance spectrum in any way.

The features obtained through proposed methods are highly dependent on the wavelets chosen for analysis (which also serve as the basis functions), unlike Fourier transform which has fixed set of basis functions. Thus, a relation cannot be found in the two methods of analysis.

Table 5.7. Detection accuracy using combination of maxima lines and ridges for the library materials.

Test Material	**Signal to noise ratio in dB**	**Percentage accuracy**	**Minimum coefficient of correlation**
HMX	9	60	0.35
HMX	10	92	0.44
HMX	11	98	0.38
HMX	12	96	0.33
HMX	13	100	0.60
HMX	14	100	0.64
PETN	9	92	0.41
PETN	15	100	0.50
PETN	16	98	0.44
PETN	17	100	0.58
PETN	17	100	0.57
RDX	7	80	0.28
RDX	8	94	0.43
RDX	9	98	0.43
RDX	10	100	0.50
RDX	11	100	0.56
TNT	9	36	0.25
TNT	10	84	0.43
TNT	11	96	0.41
TNT	12	98	0.47
TNT	13	100	0.63
TNT	14	100	0.56

Table 5.8. Improvement of classification with increasing order of wavelets using combination of maxima lines and ridges without weights and without shift.

Signal to noise ratio in dB	**Percentage accuracy**	**Minimum coefficient of correlation obtained**	**Wavelet used for analysis**
18	100	0.52	db3
17	100	0.51	db6
16	100	0.51	db10
15	100	0.52	db14
15	100	0.51	db18
14	100	0.51	db22

6 CONCLUSION

Terahertz time-domain signals from multiple target materials were tested for presence against a library of signals. The accuracy of the methods depends on the wavelets chosen and the signal to noise ratio. Different wavelets give different features of the materials, with the trend that a higher order wavelet giving more features than a lower order wavelet. As apparent from the tables in section 5, the accuracy of detection increases with the improvement in signal to noise ratio.

The CWT based methods seem to be more suitable for narrow-band signals as they result in a lesser number of scales (and hence lesser coefficients), but still providing the desired features. On the other hand, the DWT based methods provide better results when used with wide-band signals. This is due to the orthogonality of the DWT. As a result, the maximum number of coefficients used for the representation is fixed. The features available depend on the relative sub-band strengths. For a narrow-band signal, only the lower sub-bands will have appreciable energies, making the higher sub-bands less useful. Wide-band signals on the other hand would have more uniform energy distribution, thus providing more features in the limited number of coefficients available for analysis.

CWT analysis has the advantage of increasing the number of features by increasing the regularity of the wavelet, which can be used to increase the accuracy of results. CWT also provides a shift invariant analysis which may be important for real world applications. However, in applications where speed of execution is important and the time signals are not expected to shift, DWT provides a fast and efficient method for material identification.

Most of the analysis steps after the determination of the coefficients are based on logical operations (shifting, comparing, ORing, ANDing), which might be easy and efficient to implement in digital signal processors from a practical point of view.

The method used in this thesis might work better in reflective modes. The suggested method does not require signal acquisition of the pulse through the reference pellet. This is an advantage over the conventional absorption spectroscopy because the reference pellet might not always be available for material detection. Provided

that the grounded target materials with the same binding materials and pellet size, and the pulse of the same shape is radiated on the test material. The method would not require the data acquisition for the reference pellet unlike as in the absorption spectroscopy.

The disadvantage is that the results might not be consistent for pellets of varied thickness since the reference pulse gets stretched to a different degree depending on the width of the material. Consequently, the desired features will now be obtained at different scales, which will give undesirable results.

Another possible option is to use complex wavelets on the Fourier Transforms of the materials. Analysis of decibel spectrum (FFT of amplitude spectrum represented in decibels) by taking yet another Fourier transform is common in signal processing, and includes tools like cepstrum analysis, quefrency, liftering, etc. These tools are useful especially in speech processing to find out the periodicity in the amplitude spectrum. A similar approach would be to use the complex wavelets with the complex Fourier transform of the signal, which takes advantage of the absorption at particular frequencies.

APPENDIX

Description of test materials used

1. TNT is a popular explosive unaffected by ordinary shocks and must be set off by a detonator, which is favored for munitions and construction [1]. This yellow-coloured solid is sometimes used as a reagent in chemical synthesis, but it is best known as a useful explosive material with convenient handling properties. Chemically, it's known as Trinitrotoluene [19].The chemical formula is (2,4,6-trinitrotoluene).

2. PETN is a powerful explosive sensitive to shock or friction with 140% more power than TNT [1]. Chemically its known as Pentaerythritol tetranitrate. It is rarely used alone, but primarily used in booster and bursting charges of small caliber ammunition. PETN is the least stable of the common military explosives [19].

3. RDX is an explosive compound and chemically known as Cyclo-trimethylene-trinitramine. As an explosive, it is usually used in mixtures with other explosives and plasticizers, phlegmatizers or desensitizers. It is stable in storage and is considered one of the most powerful and brisant of the military high explosives. [19]. RDX is a white crystalline solid usually used in mixtures with other explosives, oils, or waxes. It has a high degree of stability in storage and is the main ingredient in plastic-bonded explosives such as C-4 [1]. The chemical formula is (1,3,5-trinitroperhydro-1,3,5-triazine).

4. HMX, also called octogen, is a powerful and relatively insensitive nitroamine high explosive, chemically related to RDX. The chemical formula is (1,3,5,7-tetranitroperhydro-1,3,5,7-tetrazocine). Because of its high molecular weight, it is one of the most powerful chemical explosives manufactured [19].

BIBLIOGRAPHY

[1] S. Kong and D. Wu, "Terahertz time-domain spectroscopy for explosive trace detection," in *IEEE International Conference on Computational Intelligence for Homeland Security and Personal Safety*, October 2006, pp. 47–50.

[2] F. Huang, B. Schulkin, H. Altan, J. F. Federici, D. Gary, R. Barat, D. Zimdars, M. Chen, and D. B. Tanner, "Terahertz study of 1,3,5-trinitro-s-triazine by time-domain and fourier transform infrared spectroscopy," *Applied Physics Letters*, vol. 85, no. 23, pp. 5535–5537, December 2004.

[3] Y. C. Shen, T. Lo, P. F. Taday, B. E. Cole, W. R. Tribe, and M. C. Kemp, "Detection and identification of explosives using terahertz pulsed spectroscopic imaging," *Applied Physics Letters*, vol. 86, no. 24, pp. 241 116–1 –241 116–3, June 2005.

[4] M. R. Leahy-Hoppa, M. Fitch, X. Zheng, L. M. Hayden, and R. Osiander, "Wide-band terahertz spectroscopy of explosives," *Chemical Physics Letters*, vol. 434, no. 4-6, pp. 227–230, September 2007.

[5] B. Ferguson, "Three dimensional t-ray inspection systems," Ph.D. dissertation, University of Adelaide, School of Electrical and Electronic Engineering, Australia, 2005. [Online]. Available: http://digital.library.adelaide.edu.au/dspace/handle/2440/37962

[6] J. Handley, A. Fitzgerald, E. Berry, and R. Boyle, "Distinguishing between materials in terahertz imaging using wide-band cross ambiguity functions," *Elsevier Journal of Digital Signal Processing*, vol. 14, no. 2, pp. 99–111, June 2004.

[7] A. B. Shah, "Terahertz data processing for standoff detection of improvised explosive devices," Master's thesis, University of Missouri-Rolla, USA, 2007.

[8] D. M. Mittleman, R. H. Jacobsen, and M. C. Nuss, "T-ray imaging," *IEEE Journal of selected topics in quantum electronics*, vol. 2, no. 3, pp. 679–692, September 1996.

[9] B. Ferguson and D. Abbott, "Wavelet de-noising of optical terahertz pulse imaging data," *Fluctuation and Noise Letters*, vol. 2, no. 1, pp. L65–L69, May 2001. [Online]. Available: http://augean.ua.oz.au/personal/dabbott/publications/FNL_ferguson2001.pdf

[10] X. X. Yin, K. M. Kong, J. W. Lim, B. W.-H. Ng, B. Ferguson, S. P. Mickan, and D. Abbott, "Enhanced t-ray signal classification using wavelet preprocessing," *Medical and Biological Engineering and Computing*, vol. 45, no. 6, pp. 611–616, June 2007.

[11] P. Du, W. A. Kibbe, and S. M. Lin, "Improved peak detection in mass spectrum by incorporating continuous wavelet transform-based pattern matching," *Oxford Journals on Bioinformatics*, vol. 22, no. 17, pp. 2059–2065, July 2006.

[12] N. Shopov, R. Ilarionov, I. Simeonov, and H. Kilifarev4, "Formation of attribute spaces using wavelets in automatic classification of explosives," in *International Conference on Computer Systems and Technologies*, vol. 1, no. 1, 2008, pp. I.1–(1–6).

[13] R. M. Rao and A. S. Bopardikar, *Wavelet Transforms: Introduction to theory and applications*. Addison-Wesley Publishers, 1998.

[14] M. Haase and J. Widjajakusumab, "Damage identification based on ridges and maxima lines of the wavelet transform," *International Journal of Engineering Science*, vol. 41, no. 13-14, pp. 1423–1443, August 2003.

[15] I. Daubechies, *Ten lectures on wavelets*. SIAM, 1992.

[16] Y. T. Chan, *Wavelet Basics*. Kluwer Academic Publishers, 1995.

[17] G. Strang and T. Nguyen, *Wavelets and filter banks*. Wellesley-Cambreidge Press, 1997.

[18] D. F. Santavicca, A. J. Annunziata, M. O. Reese, L. Frunzio, and D. E. Prober, "A far-infrared fourier transform spectrometer with an antenna-coupled niobium bolometer," *Superconductor Scienece and Technology*, vol. 20, no. 11, pp. S398–S402, October 2007. [Online]. Available: http://iopscience.iop.org/0953-2048/20/11/S19/pdf/0953-2048_20_11_S19.pdf

[19] "Trinitrotoluene, rdx, hmx, petn," January 2010. [Online]. Available: http://www.wikipedia.org/

VITA

Rajat Pashine was born in the year 1983 in Indore, a city in the central part of India. He received his Bachelors in Electronics and Instrumentation of Engineering with distinction from Shri Govindram Seksaria Institute of Technology and Science (S.G.S.I.T.S.), Indore in June 2005. He was a student member of the IEEE during this time. Following graduation, Mr. Pashine worked for two years as a Software Engineer for Infosys Technologies Ltd. at Hyderabad, India.

He then joined the Missouri University of Science and Technology (then called University of Missouri-Rolla) in August 2007 for a Master's program to pursue his interests in Electrical Engineering. He was employed as a Graduate Research Assistant and worked under Dr. Levent Acar and Dr. Vittal Rao on material identification techniques using wavelet transforms. He also served as a Graduate Teaching Assistant for different undergraduate labs at the Department of Electrical and Computer Engineering. He received his Master of Science Degree in Electrical Engineering in May 2010. Mr. Pashine is also a student member of Eta Kappa Nu, Signal Processing Society and Audio Engineering Society. His current research interests include speech, audio and image processing. He would be working with Garmin International at Olathe, State of Kansas starting February 2010.